Tumor Targeting by Covalent Conjugation of a Natural Fatty Acid to Paclitaxel

Matthews O. Bradley,[1] Nigel L. Webb, Forrest H. Anthony, Prabu Devanesan, Philip A. Witman, S. Hemamalini, Madhavi C. Chander, Sharyn D. Baker, Lifeng He, Susan Band Horwitz, and Charles S. Swindell

Protarga, Inc., King of Prussia, Pennsylvania 19406 [M. O. B., N. L. W., F. H. A., P. D., P. A. W., S. H., C. S. S.]; Department of Chemistry, Bryn Mawr College, Bryn Mawr, Pennsylvania 19010 [S. H., M. C. C., C. S. S.]; Department of Experimental Therapeutics, Johns Hopkins Oncology Center, Baltimore, Maryland 21231 [S. D. B.]; and Department of Molecular Pharmacology, Albert Einstein College of Medicine, Bronx, New York 10461 [L. H., S. B. H.]

ABSTRACT

Certain natural fatty acids are taken up avidly by tumors for use as biochemical precursors and energy sources. We tested in mice the hypothesis that the conjugation of docosahexaenoic acid (DHA), a natural fatty acid, and an anticancer drug would create a new chemical entity that would target tumors and reduce toxicity to normal tissues. We synthesized DHA-paclitaxel, a 2′-*O*-acyl conjugate of the natural fatty acid DHA and paclitaxel. The data show that the conjugate possesses increased antitumor activity in mice when compared with paclitaxel. For example, paclitaxel at its optimum dose (20 mg/kg) caused neither complete nor partial regressions in any of 10 mice in a Madison 109 (M109) s.c. lung tumor model, whereas DHA-paclitaxel caused complete regressions that were sustained for 60 days in 4 of 10 mice at 60 mg/kg, 9 of 10 mice at 90 mg/kg, and 10 of 10 mice at the optimum dose of 120 mg/kg. The drug seems to be inactive as a cytotoxic agent until metabolized by cells to an active form. The conjugate is less toxic than paclitaxel, so that 4.4-fold higher molar doses can be delivered to mice. DHA-paclitaxel in rats has a 74-fold lower volume of distribution and a 94-fold lower clearance rate than paclitaxel, suggesting that the drug is primarily confined to the plasma compartment. DHA-paclitaxel is stable in plasma, and high concentrations are maintained in mouse plasma for long times. Tumor targeting of the conjugate was demonstrated by pharmacokinetic studies in M109 tumor-bearing mice, indicating an area under the drug concentration-time curve of DHA-paclitaxel in tumors that is 8-fold higher than paclitaxel at equimolar doses and 57-fold higher at equitoxic doses. At equimolar doses, the tumor area under the drug concentration-time curve of paclitaxel derived from i.v. DHA-paclitaxel is 6-fold higher than for paclitaxel derived from i.v. paclitaxel. Even at 2 weeks after treatment, 700 nM paclitaxel remains in the tumors after DHA-paclitaxel treatment. Low concentrations of DHA-paclitaxel or paclitaxel derived from DHA-paclitaxel accumulate in gastrocnemius muscle; which may be related to the finding that paclitaxel at 20 mg/kg caused hind limb paralysis in nude mice, whereas DHA-paclitaxel caused none, even at doses of 90 or120 mg/kg. The dose-limiting toxicity in rats is myelosuppression, and, as in the mouse, little DHA-paclitaxel is converted to paclitaxel in plasma. Because DHA-paclitaxel remains in tumors for long times at high concentrations and is slowly converted to cytotoxic paclitaxel, DHA-paclitaxel may kill those slowly cycling or residual tumor cells that eventually come into cycle.

INTRODUCTION

Many anticancer drugs kill cycling cells in either the S or G_2-M phases of the cell cycle while sparing quiescent, mostly normal, cells in G_1 or G_0 (1). The fraction of a tumor's cells that are cycling at any time varies depending upon tumor type and the growth stage of the tumor. In general, faster-cycling tumors (*e.g.*, lymphomas, testicular tumors, and some childhood tumors) are more susceptible to chemotherapy than are the more common types of solid tumors with slowly cycling or noncycling cells (1). Because some normal cells such as bone marrow and intestinal mucosa also cycle rapidly, they often become dose-limiting for therapy (1).

The differences in cell kinetics between slowly and rapidly cycling tumor cells, combined with the upper dose limits imposed on antitumor drugs by proliferating normal cells, may partially explain the rather modest success that even new chemotherapeutic drugs have achieved against solid tumors.

One key to more successful chemotherapy is to find a unique property of tumor biochemistry or physiology that can be exploited to target drugs to tumors to maintain higher concentrations of cytotoxic drug for longer times and thereby create a greater therapeutic advantage. Tissue-isolated hepatomas with a single arterial inflow and a single venous outflow have been used to study the uptake of fatty acids and other metabolic precursors (2–5). In these systems, some, but not all, natural fatty acids are taken up avidly by tumors from the arterial blood, presumably for use as biochemical precursors and energy

Received 3/1/01; revised 5/29/01; accepted 6/5/01.
The costs of publication of this article were defrayed in part by the payment of page charges. This article must therefore be hereby marked *advertisement* in accordance with 18 U.S.C. Section 1734 solely to indicate this fact.

[1] To whom requests for reprints should be addressed, at Vice President of Research and Scientific Affairs, Protarga, Inc., 2200 Renaissance Boulevard, Suite 450, King of Prussia, PA 19406. Phone: (610) 592-4000; Fax: (610) 592-4001; E-mail: mbrad124@aol.com.

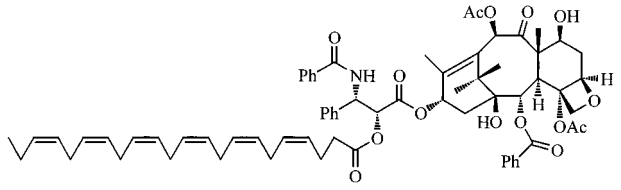

Molecular Formula: $C_{69}H_{81}NO_{15}$

Component	Molecular Weight	% of DHA-paclitaxel
DHA	328	27%
Paclitaxel	854	73%
DHA-paclitaxel	1164	100%

Fig. 1 Structure, molecular formula, and molecular weight of DHA-paclitaxel.

sources (2–5). We hypothesized that conjugating DHA,[2] a natural fatty acid, to paclitaxel might create a drug that targets tumors. We define tumor targeting to mean that the drug-fatty acid conjugate reaches higher tumor concentrations for longer times than does the unconjugated, parent drug.

To test this hypothesis, we synthesized DHA-paclitaxel, a 2′-*O*-acyl conjugate of the natural fatty acid DHA and paclitaxel (Fig. 1).

Paclitaxel, a complex taxane diterpene, was originally isolated from *Taxus brevifolia* (6, 7) and is the active compound in Taxol® which is one of the most effective and widely used anticancer drugs (6, 8). It has been approved for use in the United States against ovarian, breast, and lung cancers and Kaposi's sarcoma. It binds to β-tubulin in microtubules and stabilizes them (9, 10), thereby repressing dynamic instability (11, 12), causing the formation of parallel bundles of microtubules and inhibiting cell division at the G_2-M phase of the cell cycle (10–12).

DHA is an ω-3, C22 natural fatty acid with six *cis* double bonds. It is a constituent of cell membranes in the brain and elsewhere, and it is used as a precursor for metabolic and biochemical pathways (13, 14). DHA is found in human milk, is added to infant formula in Europe, and is classified as a nutritional additive by the United States Food and Drug Administration. On the basis of its safety, DHA and its metabolites should contribute little if any additional toxicity to paclitaxel.

MATERIALS AND METHODS

Materials

Paclitaxel was obtained from Hauser Chemical Company in Boulder, CO. DHA was obtained from Martek Biosciences Corp., Columbia, MD. GTP was purchased from Sigma Chemical Co. and dissolved in distilled water at a concentration of 100 mM for tubulin polymerization assays. MTP was prepared from calf brain by two cycles of temperature-dependent assembly-disassembly (9, 15, 16) and stored at in liquid nitrogen in MES buffer [0.1 M MES, 1 mM EGTA, and 0.5 mM $MgCl_2$ (pH 6.6)] containing 3 M glycerol. The concentration of tubulin in MTP was ~85%. Antimouse-α-tubulin monoclonal antibody was obtained from Sigma Chemical Co. All chemicals for synthetic procedures, other than DHA and paclitaxel, were obtained from Sigma Chemical Co.-Aldrich Co.

Methods

Synthesis of DHA-Paclitaxel. DHA-paclitaxel was synthesized from paclitaxel and DHA in a single step that coupled DHA to paclitaxel at the 2′-hydroxyl position. To a solution of paclitaxel (35 mg; 41 μmol) in methylene chloride (2.5 ml) under argon were added 4-dimethylaminopyridine (5 mg; 41 μmol), 1,3-dicyclohexylcarbodiimide (16.9 mg; 82 μmol), and DHA (13.5 mg; 41 μmol). The reaction mixture was stirred at ambient temperature for 2 h. After dilution with diethyl ether, the reaction mixture was washed with 5% aqueous hydrochloric acid, water, and saturated aqueous sodium chloride. The mixture was dried (sodium sulfate) and concentrated. Radial chromatography (silica gel; ethyl acetate-hexane) of the residue gave 45 mg (94%) of solid DHA-paclitaxel. In all experiments presented here, both paclitaxel and DHA-paclitaxel were formulated in 10% Cremophor EL-P/10% ethanol/80% normal saline.

Growth Inhibition in Human Tumor Cell Lines. DHA-paclitaxel was tested against a panel of 56 human tumor cell lines from a spectrum of different tumors, including leukemias, melanomas, lung, colon, central nervous system, ovarian, renal, prostate, and breast tumors, using the United States NCI screening procedures described previously (17, 18). Cell suspensions derived from each tumor cell line to be tested were inoculated into 96-well microtiter plates. Cell suspensions were preincubated for 24 h at 37°C to allow the cells to attach to the surface of the plates and to stabilize. Five concentrations of DHA-paclitaxel or paclitaxel were added to cell cultures and incubated for 48 h under standard assay conditions (17, 18). The number of cells remaining on the dish after 2 days in the continuous presence of the compound was estimated by measuring the amount of protein remaining on the plate with the sulforhodamine B assay (17, 18). These results were graphed so that the PG was plotted against the drug concentration, creating a dose-response curve. Concentrations were determined where the interpolated dose-response curves intersect at the following points: (*a*) at 50% PG, defined as growth inhibition 50; (*b*) at 0% PG, defined as total growth inhibition; and (*c*) at −50% PG, defined as lethal concentration 50. The values of growth inhibition 50, total growth inhibition, and lethal concentration 50 were calculated and used to compare the response of each cell line with each compound.

Other *in vitro* assays were performed with SKOV3, a human ovarian cancer cell line, and A549, a human non-small cell lung cancer cell line. SKOV3 was maintained in α-MEM plus ribonucleotides, deoxyribonucleotides, 15% fetal bovine serum, and 1% penicillin-streptomycin (Life Technologies, Inc.) at 37°C in 5% CO_2. A549 cells were maintained in RPMI 1640 with 10% fetal bovine serum and 1% penicillin-streptomycin (Life Technologies, Inc.) at 37°C in 7% CO_2. Cells were seeded into six-well plates at densities of 4×10^4 cells/well or 1×10^4 cells/well, respectively, and allowed to attach for 24 h, at which

[2] The abbreviations used are: DHA, docosahexaenoic acid; MTP, microtubule protein; NCI, National Cancer Institute; PG, percentage of cell growth; Pgp, P-glycoprotein; C_{max}, maximum plasma concentration; T_{max}, time to maximum concentration; AUC, area under the drug concentration-time curve; MTD, maximum tolerated dose; OD, optimum dose.

time drugs were added to each well, and the cells were incubated for an additional 72 h. Cell number was determined either by the 3-(4,5-dimethylthiazol-2-yl)-5-(3-carboxymethoxy-phenyl)-2-(4-sulfonyl)-2*H*-tetrazolium-based colorimetric method (Promega, Inc.) or with a Coulter counter.

Immunofluorescence. SKOV3 cells were grown to subconfluency on glass coverslips in 35-mm plastic Petri dishes and then incubated with drugs for 14 h. Cells were extracted with 0.5% Triton X-100 in PEM microtubule stabilizing buffer [100 mM PIPES, 2 mM EGTA, and 2 mM $MgCl_2$ (pH 6.8)] for 4 min, fixed in 3% formaldehyde in PEM for 40 min, blocked with 20% normal goat serum for 30 min and incubated with 1:100 α-tubulin monoclonal antibody for 1 h. Cy-3 conjugated goat antimouse IgG (Cappal; 1:200) was used as the secondary antibody. Samples were mounted on coverslips in 30% glycerol in PBS containing β-phenylene diamine (1 mg/ml). The presence of microtubule bundles after treatment with 100 nM of paclitaxel or 5 μM of DHA-paclitaxel was determined by observation with a Zeiss Axioskop microscope.

Tubulin Polymerization Assay. Assembly and disassembly of MTP was monitored spectrophotometrically (UVIKON; Research Instruments International, San Diego, CA) by recording changes in turbidity at 350 nm at 37°C (8, 9). MTP was diluted to 1 mg/ml in MES buffer containing 0.1 M MES, 1 mM EGTA, 0.5 mM $MgCl_2$, and 3 M glycerol (pH 6.6). GTP or the compounds to be evaluated in the absence of GTP were added to MTP and incubated at 37°C, and their turbidity was monitored as a measure of microtubule assembly (19). Aliquots were taken from each reaction and loaded onto 300-mesh electron micrograph grids for analysis on a JEOL 100 CX electron microscope at 80 kV. In the experiment, MTP (1 mg/ml) was incubated with either 1 mM GTP, 10 μM paclitaxel, or 10 μM DHA-paclitaxel at 37°C.

Cell Cycle Analysis. A549 cells were grown to subconfluency and then incubated with 5 μM of either paclitaxel or DHA-paclitaxel for 24 h. Cells were trypsinized, collected by centrifugation, resuspended, and fixed in 70% ethanol at 4°C for 1 h. After centrifugation, cells were washed twice in PBS and resuspended in 1 ml of PBS containing 20 μg/ml of propidium iodide and 5 Kunitz units of DNase-free RNase A. The samples were incubated at 37°C for 30 min and analyzed using a FACS Star Plus flow cytometer.

MDR-1 Shift Assay. The assay measures a compound's binding affinity for Pgp, one of the proteins modulating multidrug resistance. The monoclonal antibody UIC2 binds more avidly to a Pgp epitope that is altered during drug efflux. The percentage shift in PE-UIC2 fluorescence intensity in a flow cytometer was measured in the presence and absence of test compounds. The methods have been described in detail elsewhere (20–22).

Growth Inhibition of M109 and HT-29 Tumors in Mice. All animal procedures were carried out under the guidelines and approval of the animal care and use committee of the institution that performed the studies. Mice were humanely killed whenever they seemed moribund, had ulcerated tumors, or had tumors that impeded movement.

A brei (0.2 ml) of the M109 tumor, prepared from freshly harvested M109 tumors growing in mice, was inoculated s.c. into the flank of female CD2F1 mice weighing ~22 g. The M109 model and results obtained with it have been described previously (23–25). Each dose group contained 10 mice. Mice were killed whenever tumors became too large or ulcerated. Drugs were administered through the tail vein (i.v.) as a bolus once a day for 5 consecutive days at 0.1 ml/10 g body weight. Dosing of the drugs usually started on day 7 after tumor inoculation, when the tumors weighed ~65–100 mg. Each tumor was measured in two dimensions by caliper, and the recorded measurements were converted to tumor mass using the formula for a prolate ellipsoid: $[V = (a \times b^2)/2]$, where *a* is the longer, and *b* the shorter dimension.

A 1:6 homogenate of the HT-29 human colon carcinoma was implanted s.c. into female or male BALB/c-*nu/nu* mice, and mice were randomized to different treatment groups of 5 animals. DHA-paclitaxel and paclitaxel were injected into different groups of animals once a day for 5 days starting on day 14 after tumor implantation, when the median tumor volume was between 62.5 and 150 cubic mm. Compounds were administered i.p. at 0.1 ml/10 g body weight. Animal husbandry and tumor volume measurements were as above.

Measurements of DHA-Paclitaxel and Paclitaxel Concentrations in M109 Tumors, Plasma, and Gastrocnemius Muscle. The concentrations of paclitaxel and DHA-paclitaxel were measured in the tumors, plasma, and gastrocnemius muscles of female CD2F1 mice bearing M109 tumors weighing ~100 mg. Paclitaxel or DHA-paclitaxel were injected at zero time into the tail veins of mice as a single bolus. The doses injected were: 20 mg/kg of paclitaxel; 27.4 mg/kg of DHA-paclitaxel, a dose equimolar with 20 mg/kg of paclitaxel; and 120 mg/kg of DHA-paclitaxel, a dose equitoxic with 20 mg/kg of paclitaxel. Mice were killed, and tumors, plasma, and muscle were harvested as a function of time after injecting each drug. Each time point represents 10 samples from 10 different mice. Tissues were flash-frozen in liquid nitrogen and stored at −80°C.

The frozen tissues were thawed in acidified acetonitrile and homogenized, and the organic phase was extracted. This method was validated to quantitatively extract both bound and free paclitaxel and DHA-paclitaxel. The samples were loaded onto a Keystone fluorophase 5-μm column (100 mm × 2 mm) and separated by washing the column, first with 30% mobile phase A (1% acetic acid in acetonitrile) and 70% phase B [5 mM ammonium acetate (pH 6.8)] for 3 min and then a linear gradient to 95% A in 5 min at a flow rate of 0.25 ml/min. tandem mass spectrometry analysis was conducted with a PE-Sciex API 3000 Triple Quadrupole Mass Spectrometer. The eluant from the high-performance liquid chromatography was sprayed to a Turboion spray source set at 450°C, and data were collected in the positive polarity mode.

Mean plasma, muscle, and tumor concentrations at each sampling point were calculated for both DHA-paclitaxel and paclitaxel. Pharmacokinetic parameters were calculated from mean DHA-paclitaxel and paclitaxel concentration-time data using noncompartmental methods as implemented by the program WinNonlin version 2.0 (Pharsight Corp., Mountain View, CA). C_{max} and T_{max} were the observed values. The AUC was calculated using the linear trapezoidal method and was extrapolated to infinity (AUC_{inf}) by dividing the last measured concentration by the terminal rate constant, λ_z, which was deter-

mined from the slope of the terminal phase of the plasma concentration-time curve. A weighting factor of $1/C^2$ was used. The terminal half-life ($t_{1/2}$) was calculated as 0.693 divided by λ_z.

Pharmacokinetics of Paclitaxel and DHA-Paclitaxel in Rats. The plasma pharmacokinetic profiles of paclitaxel (5.0 mg/kg) and DHA-paclitaxel (6.8 mg/kg; equimolar with 5.0 mg/kg paclitaxel) were studied in male CR/CD rats. The drugs were injected into the tail vein as an infusion lasting 3 min. The plasma concentrations of paclitaxel and DHA-paclitaxel were quantitated by extracting the samples as above, and then by high-performance liquid chromatography separation using a Keystone Hypersil octadecyl silane (20 × 2 mm; 3 μm). The mobile phase solvent system consisted of 10 mM methanol/water (pH 5.5; A) and acetonitrile (B). A short, linear gradient from 5% B to 85% B in 1.4 min was used at a flow rate of 0.3 ml/min. Mass spectral analysis of the eluant was conducted on a PE-Sciex API III Plus mass spectrometer using ion spray interface in positive-ion mode.

RESULTS

NCI Human Tumor Lines

DHA-paclitaxel was tested in the 56 human tumor cell line screen of the NCI that included cell lines derived from human leukemias, melanomas, lung, colon, central nervous system, ovarian, renal, prostate, and breast tumors. A comparison of the dose-response curves for paclitaxel and DHA-paclitaxel shows that DHA conjugation lowers the cytotoxicity of DHA-paclitaxel in comparison to paclitaxel (data not shown). Whereas paclitaxel is cytotoxic to a variety of human tumor cell lines at $\sim 10^{-9}$ M, DHA-paclitaxel is active in the 10^{-6} M range.

The dose-response curves of DHA-paclitaxel in the NCI studies were summarized in a statistical analysis called "Compare Correlation." That analysis showed that microtubule agents such as vinblastine, vincristine, maytansine, and paclitaxel appeared in the list of agents most closely related to DHA-paclitaxel, which suggests that DHA-paclitaxel may also have a microtubule-based mechanism of action.

Microtubule Assembly in Solution

The assembly and disassembly of microtubule protein prepared from calf brain was monitored spectrophotometrically by recording changes in turbidity caused by incubation with either paclitaxel or DHA-paclitaxel. The results (data not shown) indicate that paclitaxel at 10 μM caused microtubule protein to assemble in the absence of GTP that is normally required for assembly, whereas DHA-paclitaxel has no effect.

Flow Cytometry Studies

A proliferating culture of A549 was incubated with 5 μM of paclitaxel or 5 μM of DHA-paclitaxel for 24 h. The cells were then fixed, stained with propidium iodide, and analyzed by FACS. The data (Fig. 2) show that both drugs arrested cell cycle progression at the G_2-M phase of the cell cycle.

Microtubule Bundle Formation as Determined by Immunofluorescence

A proliferating culture of SKOV3 cells was treated with 100 nM paclitaxel or 5 μM DHA-paclitaxel for 14 h. Cells were fixed in formaldehyde, stained with an anti-α-tubulin antibody, and examined for the formation of microtubule bundle formation by fluorescence microscopy. The photographs show that both paclitaxel (Fig. 3*B*) and DHA-paclitaxel (Fig. 3*C*) induced the formation of microtubule bundles.

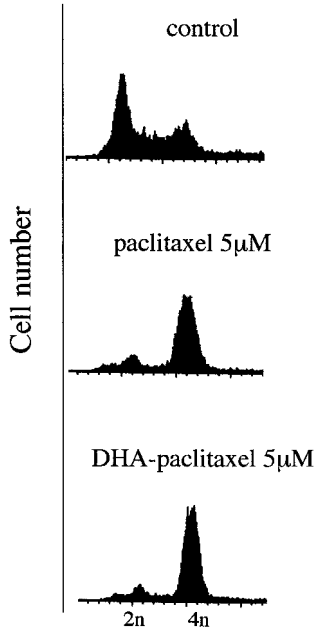

Fig. 2 DHA-paclitaxel arrests cells at the G_2-M phase of the cell cycle. A549 cells were treated with either paclitaxel or DHA-paclitaxel for 24 h before fixation and propidium iodide staining. Samples were analyzed by flow cytometry.

MDR1-Shift Assay

Table 1 shows the percentage shift in the peak of the flow cytometric profile of the phycoerythrin-labeled UIC2 fluorescence intensity in the presence and absence of test compounds in the wild-type MCF 7 cell line that does not express Pgp and in three cell lines that express increasing amounts of Pgp. The data show that DHA-paclitaxel is a relatively weak substrate for Pgp, and that paclitaxel and vinblastine are up to 4 and 13 times better substrates, respectively.

Acute Toxicity of DHA-Paclitaxel to Mice, Rats, and Dogs

The MTDs of paclitaxel and DHA-paclitaxel in mice, rats, and dogs are shown in Table 2. The dose ratio of DHA-paclitaxel to paclitaxel for the MTDs, based on taxane molarity, is 4.4 for mice, 3.6 for rats, and 2.9 for dogs. Thus, DHA-paclitaxel is much better tolerated than paclitaxel in three animal species. The dose-limiting toxicity of DHA-paclitaxel in rats and dogs was myelosuppression. At the highest doses tested, which were just sublethal, mucositis, enteropathy, atrophy of lymphoid organs, small testes, atrophy of epididymides, lower liver weights, lower terminal body weights, and increases in total cholesterol and liver transaminases were noted. These toxicities were also seen in similar acute toxicity studies of paclitaxel (6), and no new toxicities arose in the DHA-paclitaxel studies relative to those known for paclitaxel. All toxicities

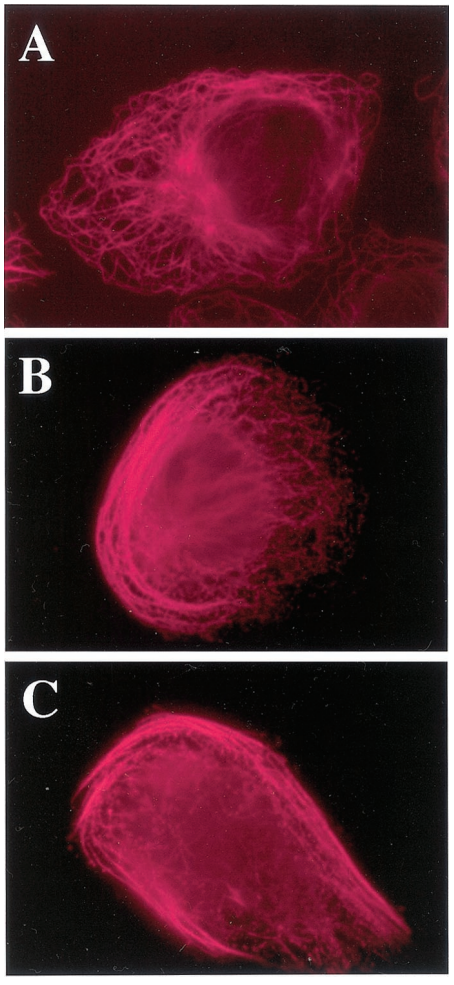

Fig. 3 Microtubule bundle formation induced by paclitaxel and DHA-paclitaxel in cultured cells. SKOV3 cells were incubated with α-tubulin antibody after exposure to paclitaxel and DHA-paclitaxel for 14 h. *A*, control (solvent); *B*, paclitaxel (100 nM); *C*, DHA-paclitaxel (5 μM).

associated with DHA-paclitaxel occurred at higher doses of taxane than with paclitaxel.

M109 Mouse Lung Tumor

Range finding studies showed that the OD, defined as the dose that causes the best therapeutic activity without formulation- or drug-related deaths, for paclitaxel in female CD2F1 mice is 20 mg/kg delivered through the tail vein once a day for 5 days. The CD2F1 mice developed hind-limb paralysis at 20 mg/kg of paclitaxel. Other investigators have delivered higher doses of paclitaxel than in our study, often by heating the drug to higher temperatures, but found no more activity than that reported at the 20 mg/kg dose (26).

The OD for DHA-paclitaxel in female CD2F1 mice is 120 mg/kg delivered through the tail vein once a day for 5 days. No mice developed hind-limb paralysis after treatment with DHA-paclitaxel.

The results show that paclitaxel did not eliminate any M109 tumors at any dose up to the OD of 20 mg/kg for 5 days

Table 1 MDR1 shift assay

The % shift refers to the changes as function of drug binding in the peak of fluorescence intensity in a flow cytometric assay for the amount of phycoerythrin-labeled UIC2 antibody bound to Pgp. Less shift means less interaction of the test compound with Pgp.

		% Shift of PE-UIC2 fluorescence intensity in the presence of drug *vs.* no drug		
Cell line	Pgp expression (molecules/cell)	DHA-paclitaxel	Paclitaxel	Vinblastine
MCF7-WT	0	0	0	0
MCF7-P4	7,500	12	38	111
MCF7-P10	14,500	44	63	72
MCF7-P19	60,000	15	65	200

(Fig. 4). The growth of the tumor was slowed for about 10 days and then continued at the same rate as the untreated control.

In contrast, DHA-paclitaxel eliminated all measurable tumor masses for 60 days in 10 of 10 mice at the OD of five daily doses of 120 mg/kg, in 9 of 10 mice at 90 mg/kg × 5 days, and in 4 of 10 mice at 60 mg/kg × 5 days (Fig. 4). Thus, DHA-paclitaxel eliminates tumors at doses that are as low as 50% and 75% of the OD.

Neither paclitaxel at its OD (20 mg/kg × 5 days; 100% of OD) nor DHA-paclitaxel at an equimolar dose (27.4 mg/kg × 5 days; 23% of OD) eliminated any tumors, although DHA-paclitaxel at 23% of its OD is as active as paclitaxel at 100% of its OD (Fig. 4).

The time course for tumor weight in individual animals (not shown) indicates that the tumors grow to about double their initial size during the 2 weeks after the five daily doses of DHA-paclitaxel treatment. Then, between one measurement and the next (usually 2–4 days), the tumors disappear, although the last drug treatment occurred 2 weeks previously. Histological analysis of the tissues in the area where the tumors had regressed at 60 days after tumor implantation showed either normal skin or the final stages of resorption of necrotic tissue but no evidence of tumor cells.

In separate experiments, neither the free acid nor the ethyl ester of DHA altered the growth curves compared with controls of the M109 tumors (data not shown). The free acid of DHA was lethal to CD2F1 mice at doses >60 mg/kg i.v. for 5 days, whereas the ethyl ester was not toxic at a dose of 120 mg/kg i.v. for 5 days. Both the free acid and the ethyl ester of DHA were formulated in 10% Cremophor EL-P/10% ethanol/80% normal saline.

HT-29

The results of the HT-29 human colon carcinoma studies are shown in Fig. 5. DHA-paclitaxel had more antitumor activity than paclitaxel in this assay. At the high dose, 100 mg/kg i.p. for 5 days, DHA-paclitaxel caused two complete responses and three partial responses of long duration of five animals. In contrast, paclitaxel at the high dose in these studies of 24 mg/kg in five mice caused only temporary growth delays and no responses at any dose and one death.

DHA-paclitaxel caused no hind-limb paralysis in the

Table 2 The MTD's of paclitaxel and DHA-paclitaxelin mice, rats, and dogs

	Dose (mg/kg)		Dose ratio: DHA-paclitaxel:paclitaxel	
Species	DHA-paclitaxel	Paclitaxel	Based on weight	Based on taxane molarity[a]
Mouse	MTD = 120 × 5 = 600	MTD = 20 × 5 = 100	6.0	4.4
Rat	Est LD_{40}[b] = 420	LD_{40} = 85	4.9	3.6
Dog	MTD = 80	Est MTD = 20	4.0	2.9

[a] MW of DHA-paclitaxel = 1164; MW of paclitaxel = 854. MW ratio of paclitaxel:DHA-paclitaxel = 0.73.
[b] LD_{40}, lithol dose at which 40% of animals die.

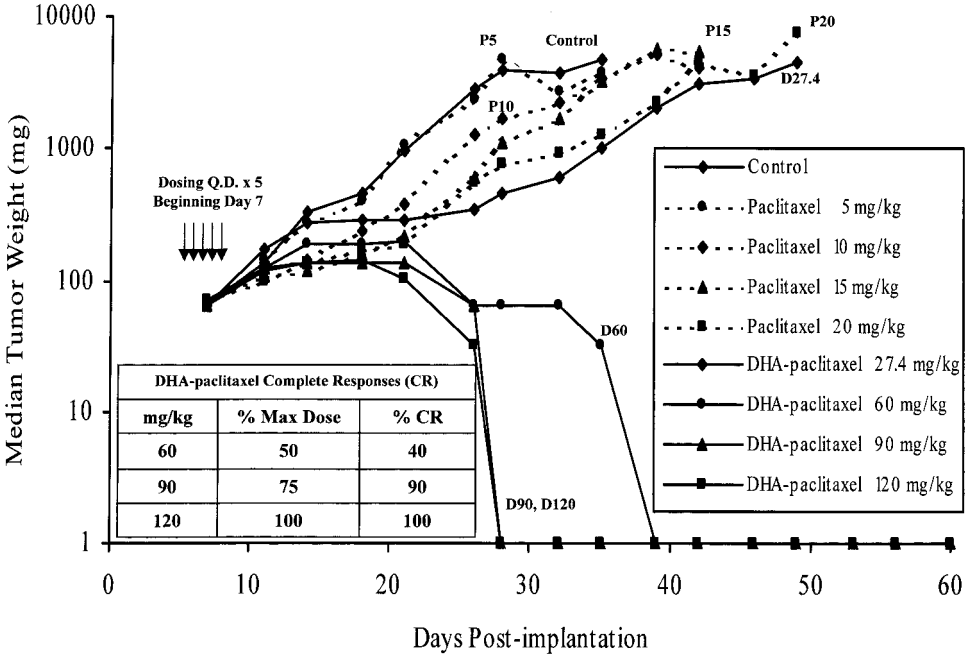

Fig. 4 Comparison of the antitumor activity of paclitaxel and DHA-paclitaxel in M109 mouse lung carcinoma. Both paclitaxel and DHA-paclitaxel were injected once a day for 5 days at the indicated daily doses in mg/kg into the tail vein of CD2F1 mice starting on day 7 after tumor inoculation, when the tumors weighed ~65 mg. The median weight of tumors from each group of 10 animals is plotted. Histological analysis of the tissues in areas where tumors had regressed showed either normal skin or the final stages of resorption of necrotic tissue.

HT-29 assay at any dose, whereas paclitaxel, at its mid- and high doses, caused severe hind-limb paralysis in some or all animals, respectively.

Pharmacokinetics of DHA-Paclitaxel

Rats. The pharmacokinetic profiles of paclitaxel (5.0 mg/kg) and DHA-paclitaxel (6.8 mg/kg) were studied in normal rats. The drugs were administered through the tail vein. Animals were killed as a function of time after injecting the drug. The volume of distribution for paclitaxel is 4.3 liters/kg and for DHA-paclitaxel, 0.058 liters/kg, which is 74-fold lower. The clearance rate for paclitaxel is 28.2 ml/min/kg, and for DHA-paclitaxel, 0.3 ml/min/kg, which is 94-fold lower. These differences suggest that most of the DHA-paclitaxel is confined within the intravascular plasma volume, whereas paclitaxel is rapidly cleared from plasma and distributed into a large volume of peripheral tissue space.

Pharmacokinetics of Paclitaxel and DHA-Paclitaxel in Tumors, Plasma, and Muscle of M109 Tumor-bearing Mice. To test the hypothesis that DHA conjugation to paclitaxel increases antitumor efficacy and decreases toxicity because of drug targeting, we studied the pharmacokinetics of paclitaxel derived from a single i.v. dose of DHA-paclitaxel in tumor-bearing mice. Paclitaxel at 20 mg/kg, DHA-paclitaxel at 27.4 mg/kg (a dose equimolar with 20 mg/kg of paclitaxel) and DHA-paclitaxel at 120 mg/kg (a dose equitoxic with 20 mg/kg of paclitaxel) were injected through the tail vein of mice bearing M109 tumors weighing ~100 mg.

As shown in Fig. 6 and Table 3, the concentration in plasma of paclitaxel derived from i.v. paclitaxel rises to a C_{max} of 42 μM within 5 min after injection and then falls quickly to <5 nM after 16 h. In contrast, paclitaxel derived from DHA-paclitaxel at an equitoxic dose of 120 mg/kg, reaches a lower C_{max} in plasma of 7.5 μM at 30 min after injection and declines more slowly. The plasma paclitaxel AUC derived from i.v. paclitaxel or DHA-paclitaxel are 34 and 61 μM × h, respectively.

The C_{max} of DHA-paclitaxel in plasma after administration of 120 mg/kg of DHA-paclitaxel is 2,595 μM at 0.5 h after injection, with a half-life of 122 h and an AUC of 12,803 μM × h (Fig. 6 and Table 3). Because the intact DHA-paclitaxel molecule has no microtubule assembly activity in cell-free so-

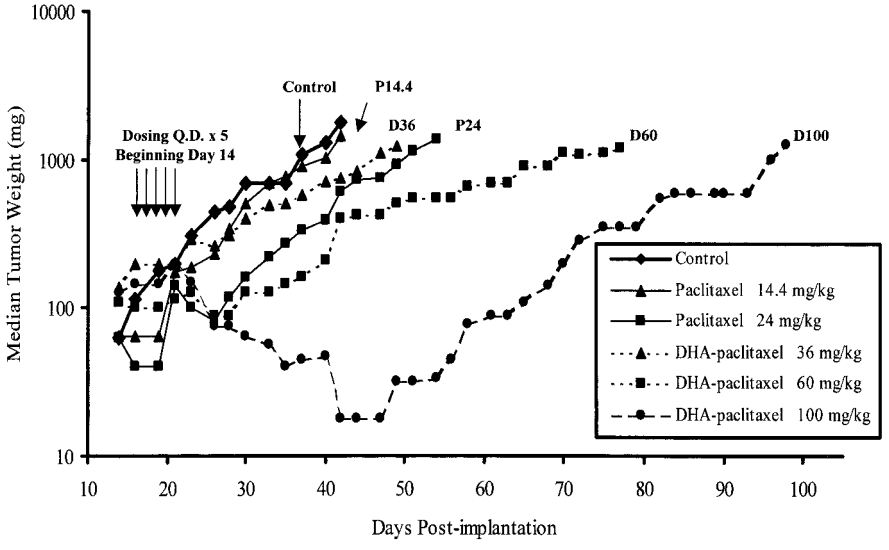

Fig. 5 Comparison of the antitumor activity of paclitaxel and DHA-paclitaxel in HT-29 human colon carcinoma cells. Both paclitaxel and DHA-paclitaxel were injected once a day for 5 days at the indicated daily doses in mg/kg into the tail vein of CD2F1mice starting on day 14 after tumor inoculation, when the tumors weighed ~100 mg. The median weight of tumors from each group of five animals is plotted.

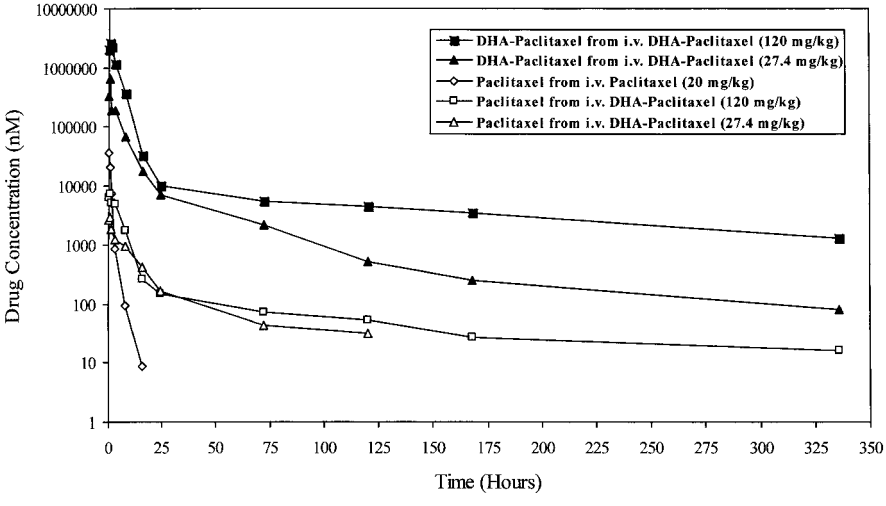

Fig. 6 Plasma:mean concentration time profiles of paclitaxel and DHA-paclitaxel in the plasma of M109 tumor-bearing mice treated with i.v. paclitaxel and i.v. DHA-paclitaxel. Both paclitaxel and DHA-paclitaxel were injected once at the indicated doses in mg/kg into the tail vein of CD2F1 mice when the tumors weighed ~100 mg. The mean concentration of each drug from 10 animals/time point is plotted. The lower limit of detection was 5 ng/ml.

lution and presumably no toxicity, we presume that the high AUCs of DHA-paclitaxel do not contribute to toxicity.

As shown in Fig. 7 and Table 3, the concentration in M109 tumors of paclitaxel derived from i.v. paclitaxel rises to a C_{max} of 9.2 μM within 30 min after injection and then falls rapidly over 24 h, becoming undetectable after 168 h. In contrast, paclitaxel derived from DHA-paclitaxel at an equitoxic dose of 120 mg/kg rises slowly to a lower C_{max} of 4.8 μM at 72 h after injection and remains high out to 336 h after injection, when 0.73 μM of paclitaxel are still present in tumors. The AUC in tumors for paclitaxel derived from i.v. paclitaxel and i.v. DHA-paclitaxel were 175 and 1013 μM × h, respectively. Thus, at equitoxic doses, DHA-paclitaxel treats M109 tumors with a 6-fold higher AUC for paclitaxel than does paclitaxel itself. Also, the time at which the concentration of paclitaxel is >2.0 μM is ~20 h for paclitaxel-derived i.v. paclitaxel, but ~240 h for paclitaxel derived from i.v. DHA-paclitaxel.

As shown in Fig. 8, DHA-paclitaxel accumulates in M109 tumors for much longer durations and at higher concentrations than paclitaxel. The AUC of DHA-paclitaxel at a 27.4 mg/kg dose in M109 tumors is 1326 μM × h, whereas that of paclitaxel at an equimolar dose of 20 mg/kg is 175 μM × h, an 8-fold increase of the AUC for DHA-paclitaxel relative to paclitaxel (Table 3). At equitoxic doses, the AUC increase is 57-fold greater for DHA-paclitaxel than for paclitaxel. Such large increases in the AUC for DHA-paclitaxel relative to paclitaxel show that DHA-paclitaxel is targeted much more specifically to tumors than is paclitaxel. The targeting of the nontoxic DHA-paclitaxel to tumors in combination with its conversion to the cytotoxic paclitaxel within the tumors, but only slightly in plasma, is consistent with the large increase in efficacy and the concomitant decrease in toxicity of DHA-paclitaxel.

Because mice treated with paclitaxel developed severe hind-limb paralysis, whereas those treated with DHA-paclitaxel at tumoricidal doses did not, we wondered whether gastrocnemius muscle would show different paclitaxel pharmacokinetics after i.v. paclitaxel and DHA-paclitaxel injections, which might account for the differences in paralysis. As shown in Fig. 9 and

Table 3 Pharmacokinetic parameters of paclitaxel (Pac) and DHA-paclitaxel (DHA-pac) in M109 tumor-bearing mice

		Plasma						Muscle						Tumor					
		C_{max}		T_{max}		AUC		C_{max}		T_{max}		AUC		C_{max}		T_{max}		AUC	
Drug	Dose (mg/kg)	Pac[a]	DHA-pac	Pac	DHA-pac	Pac	DHA-pac	Pac	DHA-pac	Pac	DHA-pac	Pac	DHA-pac	Pac	DHA-pac	Pac	DHA-pac	Pac	DHA-pac
Pac	20	42		0.083		34		7.6		0.5		22		9.2		0.5		175	
DHA-pac	27.4	3	638	0.5	0.5	29	2229	0.22	9.1	120	120	9.6	472	2	27	72	8	300	1326
DHA-pac	120	7.5	2595	0.5	0.5	61	12803	0.34	14.9	8	8	45	1576	4.8	107	72	8	1013	10028

[a] The pharmacokinetic parameters were calculated from the data in Figs. 6–9 by a model-independent method utilizing WinNonlin as described in "Materials and Methods." C_{max} is the maximum concentration achieved in μM; T_{max} is the time in hours at which C_{max} occurred: AUC is the area under the concentration-time curve, in units of μM × h in plasma, muscle, and tumor.

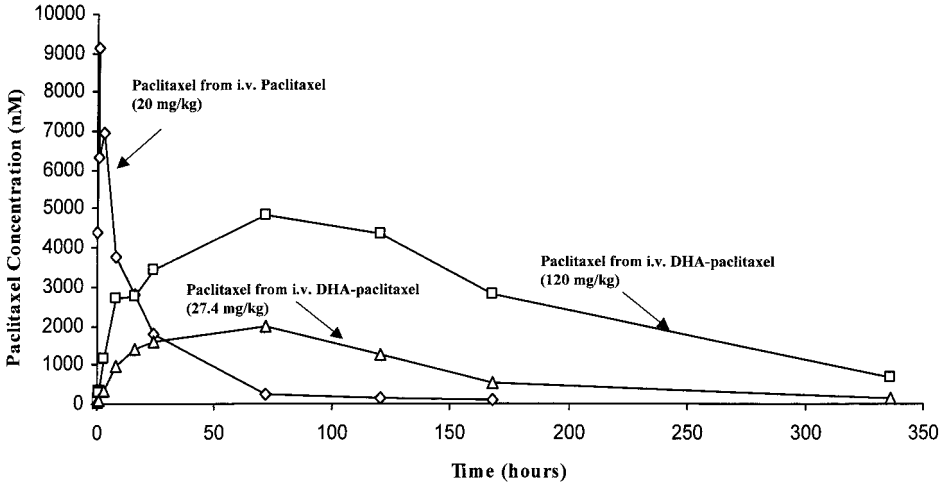

Fig. 7 Tumor:mean concentrations of paclitaxel derived from i.v. paclitaxel and i.v. DHA-paclitaxel in the tumors of M109 tumor-bearing mice treated with i.v. paclitaxel and i.v. DHA-paclitaxel. Both paclitaxel and DHA-paclitaxel were injected once at the indicated doses in mg/kg into the tail vein of CD2F1 mice when the tumors weighed ~100 mg. The mean concentration in the M109 tumors of paclitaxel derived form each drug from 10 animals/time point is plotted. The lower limit of detection was 5 ng/gm.

Table 3, the concentration in gastrocnemius muscles of paclitaxel derived from i.v. paclitaxel at 20 mg/kg rises to a C_{max} of 7.6 μM within 30 min after injection and then falls until it is undetectable after 3 days. In contrast, paclitaxel derived from DHA-paclitaxel at an equitoxic dose of 120 mg/kg rises slowly to a 22-fold lower C_{max} of 0.34 μM at 8 h after injection and then falls out to 336 h after injection (Fig. 9). The AUCs in muscle for paclitaxel derived from either 20 mg/kg i.v. paclitaxel, 27.4 mg/kg, or 120 mg/kg DHA-paclitaxel are 22, 9.6, and 45 μM × h, respectively (Table 3). Thus, the AUCs differ by about 2-fold, whereas the C_{max} values differ by 22-fold. High paclitaxel C_{max} may cause damage to the nerves innervating the muscle, which might result in hind-limb paralysis. This analysis suggests that the hind-limb paralysis may be a function of the 22-fold higher C_{max} for paclitaxel than for DHA-paclitaxel in muscle, and that low concentrations of paclitaxel for long times are better tolerated in normal, nondividing tissues.

DISCUSSION

Paclitaxel is one of the most effective cytotoxic anticancer drugs, and it is relatively water insoluble, requiring a surfactant such as Cremophor EL-P to be optimally formulated. Compared with water-soluble drugs, paclitaxel has a smaller volume of distribution and a lower clearance rate, and, as seen in Figs. 6 and 7, it is retained in tumors longer than in plasma. This modest tumor retention may account, in part, for the drug's superior antitumor efficacy compared with previous generations of antitumor drugs.

We synthesized DHA-paclitaxel with the aim of improving the targeting of paclitaxel to tumors so as to increase its efficacy and decrease its toxicity. Fatty acids are required for tumor growth and are rapidly accumulated by tumors from blood (2–5). Our hypothesis was that a conjugate of DHA, a natural fatty acid, and paclitaxel would increase the AUC of the conjugate in tumors and reduce toxicity to normal tissues. The data in this report support this hypothesis.

DHA is covalently linked to paclitaxel at the 2′-hydroxyl position. Acylation there has been shown to eliminate the microtubule assembly activity of paclitaxel (27). By attaching DHA at the 2′-position on paclitaxel, we hoped to create an inactive drug that would require hydrolysis back to paclitaxel to be cytotoxic. The *in vitro* mechanistic studies support this hypothesis. Because the conjugate has no microtubule assembly activity in solution, and yet seems by the Compare Analysis to be most closely related to other microtubule-active drugs, it is most likely that the conjugate is indeed inactive until converted to a microtubule-active agent. The flow cytometry studies show that DHA-paclitaxel, like paclitaxel, arrests cell cycle progression at the G_2-M phase of the cell cycle after 24 h. The immunofluorescence studies show that DHA-paclitaxel, also like paclitaxel, causes SKOV3 cells to form microtubule bundles after 14 h. Again, taken together, these studies support the conclusion that DHA-paclitaxel, although inactive as a microtubule agent in solution, must be converted to paclitaxel or some other active taxane within cells to be cytotoxic.

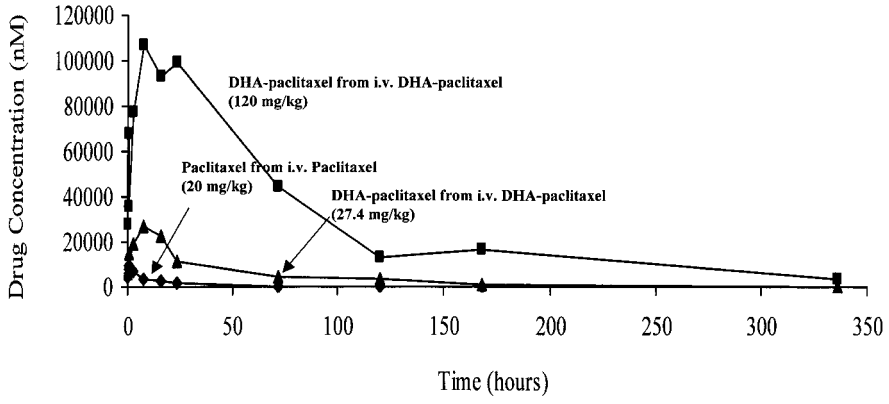

Fig. 8 Tumor:mean concentrations of paclitaxel and DHA-paclitaxel in the tumors of M109 tumor-bearing mice treated with i.v. paclitaxel and i.v. DHA-paclitaxel. Both paclitaxel and DHA-paclitaxel were injected once at the indicated doses in mg/kg into the tail vein of CD2F1 mice when the tumors weighed ~100 mg. The mean concentration in the M109 tumors of each drug from 10 animals/time point is plotted. The lower limit of detection was 5 ng/gm.

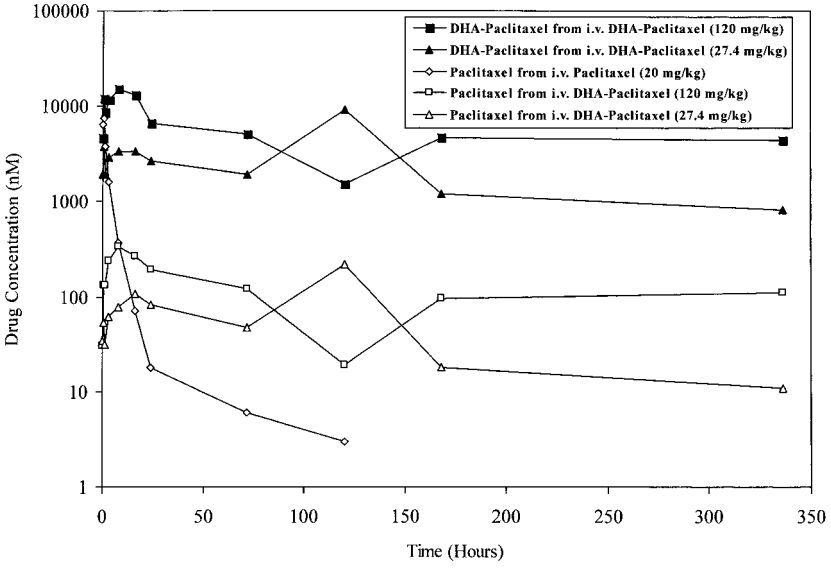

Fig. 9 Muscle:concentrations of paclitaxel and DHA-paclitaxel in the gastrocnemius muscle of M109 tumor-bearing mice treated with i.v. paclitaxel and i.v. DHA-paclitaxel. Both paclitaxel and DHA-paclitaxel were injected once at the indicated doses in mg/kg into the tail vein of CD2F1 mice when the tumors weighed ~100 mg. The mean concentration in the gastrocnemius muscle of each drug from 10 animals/time point is plotted. The lower limit of detection was 5 ng/gm.

The toxicity studies in mice, rats, and dogs (Table 2) show that DHA-paclitaxel is less toxic than paclitaxel by 3–4.4-fold on a molar basis. Yet, the dose-limiting toxicity for both drugs is myelosuppression. No new toxicities were seen with DHA-paclitaxel that have not been noted with paclitaxel. However, hind-limb paralysis in mice, presumably a predictor of peripheral neuropathy, was not seen after DHA-paclitaxel treatment at its OD but was seen after paclitaxel treatment in all animals at its OD. Because peripheral neuropathy is a significant problem with paclitaxel in clinical use (28–30), this finding in animals may translate into a significant clinical advantage for DHA-paclitaxel.

As seen in Fig. 4 and 5, DHA-paclitaxel has much greater antitumor activity than paclitaxel. In the M109 tumor model (Fig. 4), DHA-paclitaxel eliminated all palpable and histologically detectable tumors at the OD of 120 mg/kg i.v. for 5 days, whereas paclitaxel at its OD of 20 mg/kg eliminated no tumors and only slowed the tumor growth rate for about 10 days. DHA-paclitaxel also eliminated tumors in 9 of 10 mice at 90 mg/kg × 5 days and in 4 of 10 mice at 60 mg/kg × 5 days (Fig. 4). Thus, DHA-paclitaxel eliminates tumors at doses that are as low as 50% and 75% of the OD. In the HT-29 human colon carcinoma model, DHA-paclitaxel was also more active than paclitaxel, causing 2 of 5 complete responses and 3 of 5 partial responses compared with 0 of 5 responses for paclitaxel (Fig. 5).

We sought to answer the question of whether the increased antitumor activity of DHA-paclitaxel was attributable to tumor targeting and improved pharmacokinetics. To answer that question, we compared the pharmacokinetics of paclitaxel and DHA-paclitaxel in the plasma, gastrocnemius muscle, and tumors of mice bearing M109 lung tumors. The results (Table 3) show that the AUCs of DHA-paclitaxel and the paclitaxel derived from it are much higher than the AUCs of paclitaxel itself, which supports the concept that DHA conjugation to paclitaxel targets the drug to tumors.

Total AUC probably is not the only parameter that explains the greater antitumor activity of DHA-paclitaxel in comparison with paclitaxel. What may be of more importance is the much longer time at which the concentration of paclitaxel remains

high in tumors after DHA-paclitaxel than after paclitaxel. For example, paclitaxel remains above 2 μM in tumors for only 16 h after 20 mg/kg of i.v. paclitaxel, whereas paclitaxel derived from 120 mg/kg of i.v. DHA-paclitaxel remains above 2 μM for ~240 h (Fig. 7). Tumors started to grow once the concentration of paclitaxel, derived either from paclitaxel or DHA-paclitaxel, fell to below about 2 μM (data not shown), so this concentration may be critical for antitumor activity. Because most cells in a tumor are in G_1 or G_0 during any 16-h period, they will survive paclitaxel treatment. In contrast, with DHA-paclitaxel maintaining concentrations of paclitaxel >2 μM for 240 h, many of the cells in even a slow-growing tumor will come into the cell cycle during that time and be killed. The concentrations of DHA-paclitaxel and paclitaxel were measured in tumors after a single i.v. dose. Repeated doses would be expected to produce even higher intratumor concentrations.

The decreased dose-limiting toxicity and hind-limb paralysis of DHA-paclitaxel compared with paclitaxel also may be explained by the pharmacokinetic studies. Although the AUC in plasma of paclitaxel derived from DHA-paclitaxel at 120 mg/kg is almost twice that of paclitaxel at 20 mg/kg, the C_{max} is 5.5-fold less (Table 3), yet the dose-limiting toxicities of myelosuppression are similar. In muscle, where the AUC of paclitaxel derived from DHA-paclitaxel at 120 mg/kg is about twice that of the AUC of paclitaxel at 20 mg/kg, the C_{max} is 22-fold less (Table 3). Yet paclitaxel causes hind-limb paralysis, and DHA-paclitaxel does not. One conclusion from these results is that peripheral nerve toxicity is more closely related to C_{max} than to AUC, especially when the higher AUC is caused by low concentrations of drug for longer periods of time.

In conclusion, the conjugation of DHA to paclitaxel creates a new chemical entity, DHA-paclitaxel, that targets syngeneic and xenogeneic tumors in mice and results in less toxicity and more therapeutic efficacy. DHA-paclitaxel has entered full clinical development, a Phase I study has been completed, and a number of Phase II studies for different cancers have begun.

REFERENCES

1. Tannock, I. F. Principles of cell proliferation: cell kinetics. *In:* V. T. DeVita, Jr., S. Hellman, S. A. Rosenberg (eds.), Cancer: Principle and Practice of Oncology, Ed. 3, pp. 3–13. Philadelphia: J. B. Lippincott, Philadelphia, 1989.

2. Sauer, L. A., Nagel, W. O., Dauchy, R. T., Miceli, L. A., and Austin, J. E. Stimulation of tumor growth in adult rats *in vivo* during an acute fast. Cancer Res., *46:* 3469–3475, 1986.

3. Sauer, L. A., Stayman, J. W., III, and Dauchy, R. T. Amimo acid, glucose, and lactic acid utilization by rat tumors. Cancer Res., *42:* 4090–4097, 1982.

4. Sauer, L. A., and Dauchy, R. T. Tumour-host metabolic interrelationships. Biochem. Soc. Trans., *18:* 80–82, 1990.

5. Sauer, L. A., and Dauchy, R. T. The effect of ω-6 and ω-3 fatty acids on ^{3}H-thymidine incorporation in hepatoma 7288CTC perfused *in situ*. Brit. J. Cancer, *66:* 297–303, 1992.

6. Suffness, M. (ed.). Taxol® Science and Applications, pp.3–416. Boca Raton, FL: CRC Press, Inc., 1995.

7. Wani, M. C., Taylor, H. L., Wall, M. E., Coggon, P., and McPhail, A. T. Plant antitumor agents. VI. The isolation and structure of Taxol, a novel antileukemic and antitumor agent from *Taxus brevifolia*. J. Am. Chem. Soc., *93:* 2325–2327, 1971.

8. McGuire, W. P., Rowinsky, E. K., Rosenshein, N. B., Grumbine, F. C., Ettinger, D. S., Armstrong, D. K., and Donehower, R. C. Taxol: a unique antineoplastic agent with significant activity in advanced ovarian epithelial neoplasms. Ann. Intern. Med., *111:* 273–279, 1989.

9. Schiff, P. B., Fant, J., and Horwitz, S. B. Promotion of microtubule assembly. *In vitro* by Taxol. Nature (Lond.), *277:* 665–667, 1979.

10. Schiff, P. B., Fant, J., and Horwitz, S. B. Taxol stabilizes microtubules in mouse fibroblast cells. Proc. Natl. Acad. Sci. USA, *77:* 1561–1565, 1980.

11. Yvon, A. M., Wadsworth, P., and Jordan, M. A. Taxol suppresses dynamics of individual microtubules in living human tumor cells. Mol. Biol. Cell, *10:* 947–949, 1999.

12. Jordan, M. A., Toso, R. J., Thrower, D., and Wilson, L. Mechanism of mitotic block and inhibition of cell proliferation by Taxol at low concentrations. Proc. Natl. Acad. Sci. USA, *90:* 9552–9556, 1993.

13. Anderson, G. J., Connor, W. E., and Corliss, J. D. Docosahexaenoic acid is the preferred dietary n-3 fatty acid for the development of the brain and retina. Pediatr. Res., *27:* 89–97, 1990.

14. Connor, W. E., and Neuringer, M. The effects of n-3 fatty acid deficiency and repletion upon the fatty acid composition and function of the brain and retina. Prog. Clin Biol. Res., *282:* 275–294, 1988.

15. Schiff, P. B., and Horwitz, S. B. Taxol assembles tubulin in the absence of exogenous guanosine 5′-triphosphate or microtubule-associated proteins. Biochemistry, *20:* 3247–3252, 1981.

16. Weisenberg, R. C. Microtubule formation *in vitro* in solutions containing low calcium concentrations. Science (Wash. DC), *177:* 1104–1105, 1972.

17. Monks, A., Scudiero, D., Skehan, P., Shoemaker, K. P., Vistica, D., Hose, C., Langley, J., Cronise, P., Vaigro-Wolff, A., Gray-Goodrich, M., Campbell, H., Mayo, J., and Boyd, M. Feasibility of a high-flux anticancer drug screen using a diverse panel of cultured human tumor cell lines. J. Natl. Cancer Inst., *83:* 757–765, 1991.

18. Boyd, M. R. The NCI *in vitro* anticancer drug discovery screen: concept, implementation, and operation. *In:* B. Teicher (ed.), Anticancer Drug Development Guide: Preclinical Screening, Clinical Trials, and Approval, pp. 23–42. Totowa, NJ: Humana Press, 1996.

19. Shelanski, M. L., Gaskin, F., and Cantor, C. R. Microtubule assembly in the absence of added nucleotides. Proc. Natl. Acad. Sci. USA, *70:* 765–768, 1993.

20. Mechetner, E. B., and Roninson, I. B. Efficient inhibition of P-glycoprotein-mediated multidrug resistance with a monoclonal antibody. Proc. Natl. Acad. Sci. USA, *89:* 5824–5828, 1992.

21. Mechetner, E. B., Schott, B., Morse, B., Stein, W. D., Druley, T., Davis, K. A., Tsuruo, T., and Roninson, I. B. P-glycoprotein function involves conformational transitions detectable by differential immunoreactivity. Proc. Natl. Acad. Sci. USA, *94:* 12908–12913, 1997.

22. Mechetner, E. B., Kyshtoobayeva, A., Zonis, S., Kim, H., Stroup, R., Garcia, R., Parker, R., J., and Fruehauf, J. P. Levels of multidrug resistance (MDR1) P-glycoprotein expression by human breast cancer correlate with *in vitro* resistance to Taxol and doxorubicin. Clin. Cancer Res., *4:* 389–398, 1998.

23. Rose, W. C. Evaluation of Madison 109 lung carcinoma as a model for screening antitumor drugs. Cancer Treat. Rep., *65:* 299–312, 1981.

24. Rose, W. C. Taxol-based combination chemotherapy and other *in vivo* preclinical antitumor studies. J. Natl. Cancer Inst. Monogr., *15:* 47–53, 1993.

25. Rose, W. C. Preclinical antitumor activity of taxanes. *In:* Suffness, M. (ed.), Taxol®: Science and Applications, pp. 209–235. Boca Raton, FL: CRC Press, Inc., 1995.

26. Fujita, H., Okamoto, M., Takao, A., Mase, H., and Kojima, H. Pharmacokinetics of palitaxel in experimental animals. Jpn. J. Cancer Chemother., *21:* 659–664, 1994.

27. Mellado, W. Preparation and biological activity of Taxol acetates. Biochem. Biophys. Res. Commun., *124:* 329–336, 1984.

28. Jordan, M., A., Wendell, K., Gardiner, S., Derry, W. B., Copp, H., and Wilson, L. Mitotic block induced in HeLa cells by low concentrations of paclitaxel (Taxol) results in abnormal mitotic exit and apoptotic cell death. Cancer Res., *56:* 816–825, 1996.

29. Hilkens, P., H., and ven den Bent, M., J. Chemotherapy-induced peripheral neuropathy. J. Peripher. Nerv. Syst., *2:* 350–361, 1997.

30. Iniquez, C., Larrode, P., Mayordomo, J. I., Gonzalez, P., Adelantado, S., Yubero, A., Tres, A., and Morales, F. Reversible peripheral neuropathy induced by a single administration of high-dose paclitaxel. Neurology, *51:* 868–870, 1998.